

Minimal model dependent constraints on cosmological nuisance parameters from combinations of cosmological data

Bikash R. Dinda ^{1,*}

¹ *Department of Physical Sciences, Indian Institute of Science Education and Research Kolkata, India.*

The study of cosmic expansion history and the late time cosmic acceleration from observational data depends on the nuisance parameters associated with the data. For example, the absolute peak magnitude of type Ia supernova associated with the type Ia supernova observations and the comoving sound horizon at the baryon drag epoch associated with baryon acoustic oscillation observations are two nuisance parameters. The nuisance parameters associated with the quasar and the gamma-ray bursts data are also considered. These nuisance parameters are constrained by combining the cosmological observations using the Gaussian process regression method without assuming any cosmological model or parametrization to the background cosmic expansion. The bounds obtained in this method can be used as the prior for the data analysis while considering the observational data accordingly. Interestingly, these bounds are independent of the present value of the Hubble parameter. Along with these nuisance parameters, the cosmic curvature density parameter is also constrained simultaneously and the constraints show no significant deviation from a flat Universe.

PACS numbers:

Introduction- The late time cosmic acceleration is one of the major discoveries in the late 20th century [1–4]. This acceleration has been confirmed by several cosmological observations such as type Ia supernova [5–8], cosmic microwave background (CMB) [9–11], baryon acoustic oscillation (BAO) [12–14] etc. One of the possible explanations of the late time cosmic acceleration is the introduction of an exotic matter component, called dark energy, that has large negative pressure [15–17]. Another alternative to explain this acceleration is the modification of general relativity at large cosmological scales [18–21]. Several dark energy and modified gravity models have been proposed in the literature and these models have been constrained and shaped by the cosmological observations [21, 22].

Alongside the type Ia supernova, CMB, and BAO observations, several other observations have been continuously developed to better understand the nature of the late time cosmic acceleration and the mechanisms to explain this acceleration. For example, such observations are the cosmic chronometers (CC) [23, 24], Quasar (QSO) [25–27], and gamma-ray bursts (GRB) [28–30] observations. All these recent observations are providing us with percent precision data which are helpful to understand the nature of dark energy or modification of gravity [31, 32] with high precision.

The simplest candidate for dark energy is considered to be the cosmological constant and the corresponding model is called the Λ CDM model [33]. This is the most successful model to study the evolution of the Universe in light of recent cosmological observations [9–11].

This model has theoretical problems like fine-tuning and cosmic coincidence problems [34–37]. Despite these theoretical problems, there are other inconsistencies with this model that arose from the percent precision observational data [38, 39]. One such example is the so-called Hubble tension [40–42]. Considering these caveats into account, it is necessary to go beyond the Λ CDM model. In this context, in literature, many dynamical dark energy and modified gravity models have been developed gradually [21, 22].

The background dynamics of the Universe are not only studied through different dark energy and modified gravity models, it has been studied through different parametrizations to the different cosmological quantities without assuming any model [43–48]. Even in recent times, background dynamics are studied from several observations without assuming any model or parametrization by using various modern techniques [49–54]. One such technique is the Gaussian process regression (GPR) and it has been used in the literature in several contexts [55–57]. The GPR method is the key ingredient in our analysis.

Most of the above-mentioned observations involve cosmological nuisance parameters like the peak absolute magnitude of the type Ia supernova [58, 59]. Because of this reason, the model independent studies of the late time cosmic acceleration depend on these cosmological nuisance parameters [60, 61]. So, to study the late time cosmic acceleration, we need prior information on these parameters. However, without priors or with flat priors, these parameters can be constrained by combining differ-

ent observations [62]. In our analysis, we constrain these nuisance parameters from the joint analysis of cosmological observations, mentioned above.

Methodology- In our entire analysis, we assume that the geometry of the Universe is described by the Friedmann-Lemaître-Robertson-Walker (FLRW) metric. The luminosity distance d_L is related to the relative peak magnitude, m of the type Ia supernova observations given as

$$m - M_B = 5 \log_{10} \left(\frac{d_L}{\text{Mpc}} \right) + 25, \quad (1)$$

where M_B is the absolute peak magnitude of the type Ia supernova. The type Ia supernova observations measure m with some error bars (Δm) [7]. We consider the notation ΔX to represent the standard deviation in X throughout this analysis. For the type Ia supernova observations, we consider Pantheon compilation data [7]. Thus, the luminosity distance is obtained from the observed m using the above equation given as

$$d_L = 10^{\frac{1}{5}(m-25-M_B)} \text{ Mpc}. \quad (2)$$

And we get corresponding standard deviations in the luminosity distance using propagation of uncertainty through Eq. (2). However, from Eq. (2), we can see that the determination of d_L and Δd_L depends on M_B . We determine this M_B parameter by combining the type Ia supernova and cosmic chronometers (CC) observations. CC observations have the data for the Hubble parameter with corresponding standard deviations [23, 24]. The Hubble parameter, H is related to m and its derivative (m') via d_L and its derivative (d'_L) given as

$$H = \left(\frac{(1+z)^2 [c^2(1+z)^2 + W_{k0}d_L^2]}{[(1+z)d'_L - d_L]^2} \right)^{\frac{1}{2}}, \quad (3)$$

where z is the redshift, c is the speed of light in vacuum, and W_{k0} is given as

$$W_{k0} = \Omega_{k0}H_0^2 = 10^4 (\Omega_{k0}h^2) [\text{KmS}^{-1}\text{Mpc}^{-1}]^2, \quad (4)$$

where Ω_{k0} is the cosmic curvature density parameter and H_0 is the present value of the Hubble parameter and it is related to the dimensionless parameter, h as

$H_0 = 100h\text{KmS}^{-1}\text{Mpc}^{-1}$. Thus the reconstruction of the Hubble parameter from the type Ia supernova data depends on the M_B and W_{k0} parameters. From Eq. (3), we can see that the determination of H also depends on m' via d'_L . Using Eq. (2), d'_L is computed from m' given as

$$d'_L = \frac{\log 10}{5} m' 10^{\frac{m-M_B-25}{5}} \text{ Mpc}, \quad (5)$$

So, putting Eqs. (2) and (5) in Eq. (3), we can determine the Hubble parameter from m and m' as a function of M_B and W_{k0} parameters. Similarly, we can determine the corresponding standard deviations in the Hubble parameter through error propagation. We compare the reconstructed Hubble parameter from type Ia supernova data with the Hubble parameter data obtained directly from the CC data to determine M_B and W_{k0} simultaneously.

However, the reconstruction of the Hubble parameter from type Ia supernova (SN) data and the comparison to the CC data is not straightforward because the SN data provide the observations only of m , not of m' and these data are not at the same redshift points as in the CC data. These issues are solved by using the Gaussian process regression (GPR) analysis because using GPR, one can get a quantity and its derivative at some target points from the actual data which have the quantity at some different points. For example, here, we get m , m' , Δm and $\Delta m'$ at CC redshift points (z_{CC}) from m and Δm at SN redshift points (z_{SN}). For the details of GPR see [55–57]. Note that GPR analysis requires a kernel function and a mean function which involve some parameters. Here, we consider the squared exponential kernel. For the mean function, we consider the Λ CDM model. We marginalize the parameters involved in these functions in GPR analysis to reduce the model dependence. After marginalization, this model dependence is not very significant. For details see [57].

From reconstructed m , m' , Δm and $\Delta m'$ at z_{CC} , we obtain H and ΔH at z_{CC} using above equations and uncertainty propagation. We denote these as H_{SN} and ΔH_{SN} respectively. We denote the Hubble parameter and the corresponding standard deviation from CC data as H_{CC} and ΔH_{CC} respectively. We compare H_{SN} and H_{CC} to obtain constraints on M_B and W_{k0} simultaneously by maximizing the log-likelihood ($\log L_{CC+SN}$) given as

$$\log L_{CC+SN}(M_B, W_{k0}) = -\frac{1}{2} \sum_{z_{CC}} \frac{[H_{SN}(M_B, W_{k0}) - H_{CC}]^2}{\Delta H_{tot}^2(M_B, W_{k0})} - \frac{1}{2} \sum_{z_{CC}} \log [2\pi \Delta H_{tot}^2(M_B, W_{k0})], \quad (6)$$

where ΔH_{tot}^2 is the total variance in the Hubble parameter given as $\Delta H_{tot}^2(M_B, W_{k0}) = \Delta H_{SN}^2(M_B, W_{k0}) + \Delta H_{CC}^2$.

The BAO data have two kinds of measurements: one is in the line of sight direction and related to the quantity, D_H ; the second one is in the transverse direction and related to the quantity, D_M . D_H and D_M are given as

$$D_H = \frac{1}{r_d} \frac{c}{H}, \quad (7)$$

$$D_M = \frac{1}{r_d} \frac{d_L}{1+z}, \quad (8)$$

where r_d is the comoving sound horizon at baryon drag epoch [13]. We determine the r_d parameter by combining the BAO data with the SN and CC data as follows: Using GPR, we reconstruct D_H and the corresponding errors as functions of r_d at BAO redshift points (z_{BAO}) from the CC data. We denote these as D_H^{CC} and ΔD_H^{CC} respectively. We compare these with the D_H directly obtained from the BAO data and we denote this as D_H^{BAO} . We denote the corresponding errors as ΔD_H^{BAO} . The corresponding log likelihood ($\log L_{CC+BAO1}$) is defined as

$$\log L_{CC+BAO1}(r_d) = -\frac{1}{2} \sum_{z_{BAO}} \frac{[D_H^{CC}(r_d) - D_H^{BAO}]^2}{(\Delta D_H^{tot}(r_d))^2} - \frac{1}{2} \sum_{z_{BAO}} \log [2\pi (\Delta D_H^{tot}(r_d))^2], \quad (9)$$

where $(\Delta D_H^{tot})^2$ is the total variance in D_H given as $(\Delta D_H^{tot}(r_d))^2 = (\Delta D_H^{CC}(r_d))^2 + (\Delta D_H^{BAO})^2$.

Similarly, we can define a log-likelihood ($\log L_{SN+BAO2}$) for the second kind of BAO data by comparing D_M obtained directly from BAO and the reconstructed one from SN data using GPR given as

$$\log L_{SN+BAO2}(M_B, r_d) = -\frac{1}{2} \sum_{z_{BAO}} \frac{[D_M^{SN}(M_B, r_d) - D_M^{BAO}]^2}{(\Delta D_M^{tot}(M_B, r_d))^2} - \frac{1}{2} \sum_{z_{BAO}} \log [2\pi (\Delta D_M^{tot}(M_B, r_d))^2], \quad (10)$$

where D_M^{SN} is the reconstructed D_M obtained from SN data at BAO redshift points using GPR, D_M^{BAO} is D_M obtained directly from the BAO data, and $(\Delta D_M^{tot})^2$ is

the total variance in D_M given as $(\Delta D_M^{tot}(M_B, r_d))^2 = (\Delta D_M^{SN}(M_B, r_d))^2 + (\Delta D_M^{BAO})^2$, where ΔD_M^{SN} are the reconstructed errors from SN and ΔD_M^{BAO} are the errors from BAO data.

In quasar observations (QSO), the data have simultaneous measurements in X-ray flux (F_X) and ultraviolet (UV) ray flux (F_{UV}) [25–27]. These are related to the luminosity distance given as

$$Q = \log_{10} F_X = \beta + (\gamma - 1) \log_{10}(4\pi) + \gamma \log_{10} F_{UV} + 2(\gamma - 1) \log_{10} d_L, \quad (11)$$

where β and γ are two nuisance parameters. From SN data, using GPR, we reconstruct Q and the corresponding standard deviations as functions of M_B , β , and γ at QSO redshift points (z_{QSO}). We denote this as Q_{SN} . We denote Q obtained directly from QSO data as Q_{QSO} . Comparing these two, we constrain M_B , β , and γ simultaneously by defining a log-likelihood ($\log L_{SN+QSO}$) given as

$$\log L_{SN+QSO}(M_B, \beta, \gamma, \delta) = -\frac{1}{2} \sum_{z_{QSO}} \frac{[Q_{SN}(M_B, \beta, \gamma) - Q_{QSO}]^2}{\Delta Q_{tot}^2(M_B, \beta, \gamma) + \delta^2} - \frac{1}{2} \sum_{z_{QSO}} \log [2\pi (\Delta Q_{tot}^2(M_B, \beta, \gamma) + \delta^2)], \quad (12)$$

where δ is another nuisance parameter accounted in the total variance in Q (denoted by ΔQ_{tot}^2) while considering QSO data. ΔQ_{tot}^2 is given by $\Delta Q_{tot}^2(M_B, \beta, \gamma) = \Delta Q_{SN}^2(M_B, \beta, \gamma) + \Delta Q_{QSO}^2$. Here Q_{SN} and ΔQ_{SN} are the reconstructed Q and the corresponding errors from the SN data using GPR respectively. Q_{QSO} and ΔQ_{QSO} correspond to Q and the corresponding errors, obtained directly from the QSO data respectively.

The Amati correlated gamma-ray bursts (GRB) data have simultaneous measurements in the observed peak energy, E_p^{obs} of GRB photons and bolometric fluence, S_{bolo} [28–30]. These quantities are related to the luminosity distance through Amati relations given by

$$P = \log \left(\frac{E_{iso}}{\text{erg}} \right) = a + b \log \left(\frac{E_p}{\text{keV}} \right), \quad (13)$$

$$E_{iso} = 4\pi d_L^2 S_{bolo} (1+z)^{-1}, \quad (14)$$

$$E_p = E_p^{obs} (1+z), \quad (15)$$

where E_{iso} is the isotropic energy and E_p is the rest-frame peak energy of GRB photons; a and b are two nuisance parameters involved in the GRB observations. Using Eqs. (2) and (14), we can compute P from m and the corresponding errors through error propagation as functions of M_B . Using GPR, we reconstruct P from SN data at GRB redshift points (z_{GRB}) and denote this as P_{SN} . We denote the corresponding errors as ΔP_{SN} . We also compute P from GRB data at the same redshift points as functions of a and b using Eqs. (13) and (15). We denote this as P_{GRB} . We denote the corresponding errors as ΔP_{GRB} . We simultaneously constrain M_B , a , and b by defining a log-likelihood ($\log L_{\text{SN+GRB}}$) defined as

$$\begin{aligned} & \log L_{\text{SN+GRB}}(M_B, a, b, \sigma_{\text{ext}}) \\ &= -\frac{1}{2} \sum_{z_{\text{GRB}}} \frac{[P_{\text{SN}}(M_B) - P_{\text{GRB}}(a, b)]^2}{\Delta P_{\text{tot}}^2(M_B, b) + \sigma_{\text{ext}}^2} \\ & - \frac{1}{2} \sum_{z_{\text{GRB}}} \log [2\pi(\Delta P_{\text{tot}}^2(M_B, b) + \sigma_{\text{ext}}^2)], \quad (16) \end{aligned}$$

where σ_{ext} is another nuisance parameter involved in the GRB observations through the total variance in P (denoted by ΔP_{tot}^2). ΔP_{tot}^2 is given by $\Delta P_{\text{tot}}^2(M_B, b) = \Delta P_{\text{SN}}^2(M_B) + \Delta P_{\text{GRB}}^2(b)$.

Thus we get simultaneous constraints on M_B and W_{k0} from combinations of CC and SN data by maximizing the log-likelihood mentioned in Eq. (6). Next, we get simultaneous constraints on M_B , W_{k0} , and r_d from combinations of CC, SN, and BAO data by maximizing the log-likelihood ($\log L_{\text{CC+SN+BAO}}$) given as

$$\begin{aligned} \log L_{\text{CC+SN+BAO}}(M_B, W_{k0}, r_d) &= \log L_{\text{CC+SN}}(M_B, W_{k0}) \\ &+ \log L_{\text{CC+BAO1}}(r_d) + \log L_{\text{SN+BAO2}}(M_B, r_d). \quad (17) \end{aligned}$$

Further, we get simultaneous constraints on M_B , W_{k0} , r_d , β , γ , and δ from the combinations of CC, SN, BAO, and QSO data by maximizing the log-likelihood ($\log L_{\text{CC+SN+BAO+QSO}}$) given as

$$\begin{aligned} \log L_{\text{CC+SN+BAO+QSO}}(M_B, W_{k0}, r_d, \beta, \gamma, \delta) \\ &= \log L_{\text{CC+SN+BAO}}(M_B, W_{k0}, r_d) \\ &+ \log L_{\text{SN+QSO}}(M_B, \beta, \gamma, \delta). \quad (18) \end{aligned}$$

Similarly, we get simultaneous constraints on M_B , W_{k0} , r_d , a , b , and σ_{ext} from the combinations of CC, SN,

BAO, and GRB data by maximizing the log-likelihood ($\log L_{\text{CC+SN+BAO+GRB}}$) given as

$$\begin{aligned} \log L_{\text{CC+SN+BAO+GRB}}(M_B, W_{k0}, r_d, a, b, \sigma_{\text{ext}}) \\ &= \log L_{\text{CC+SN+BAO}}(M_B, W_{k0}, r_d) \\ &+ \log L_{\text{SN+GRB}}(M_B, a, b, \sigma_{\text{ext}}). \quad (19) \end{aligned}$$

Finally, we can add the CMB data to tighten the constraints on the nuisance parameter. We use Gaussian prior on r_d obtained from the results of the Planck 2018 mission given as $r_d = 147.09 \pm 0.26$ [11]. We do not use full likelihood from Planck, because this result is almost independent of the late time dynamics. We define a log-likelihood ($\log L_{\text{CMB}}$) corresponding to this Gaussian prior given as

$$\log L_{\text{CMB}}(r_d) = -\frac{1}{2} \frac{(r_d - 147.09)^2}{0.26^2} - \frac{1}{2} \log(2\pi \cdot 0.26^2). \quad (20)$$

To add CMB data to any combination of data, we add the CMB log-likelihood to the one corresponding to that combination.

Results and conclusion- The constraints on the nuisance parameters are dependent on the constraints on the W_{k0} parameter that is related to $\Omega_{k0}h^2$ through Eq. (4). We quote all the results through $\Omega_{k0}h^2$ parameter instead of W_{k0} .

In Figure 1, we have shown constraints on $\Omega_{k0}h^2$, r_d , and M_B parameters obtained from different combinations of data. The dashed-red, dotted-blue, and solid-black lines correspond to the constraints obtained from CC+SN, CC+SN+BAO, and CC+SN+BAO+CMB combinations of data respectively. For CC+SN, we obtain constraints only on $\Omega_{k0}h^2$ and M_B not on r_d . Addition of BAO data put constraints on r_d along with $\Omega_{k0}h^2$ and M_B . For this case, constraints on $\Omega_{k0}h^2$ and M_B are comparatively tighter. Further, the addition of CMB data corresponds to the tightest constraints on these parameters. The values of these constraints are mentioned in Table I.

In Figure 2, we have shown constraints on the QSO nuisance parameters, β , γ , and δ for two different combinations of data. The blue-dotted and solid-black lines correspond to CC+SN+BAO+QSO and CC+SN+BAO+QSO+CMB combinations of data respectively. We have not explicitly shown the constraints on $\Omega_{k0}h^2$, r_d , and M_B parameters because these constraints are very similar to those in the previous figure.

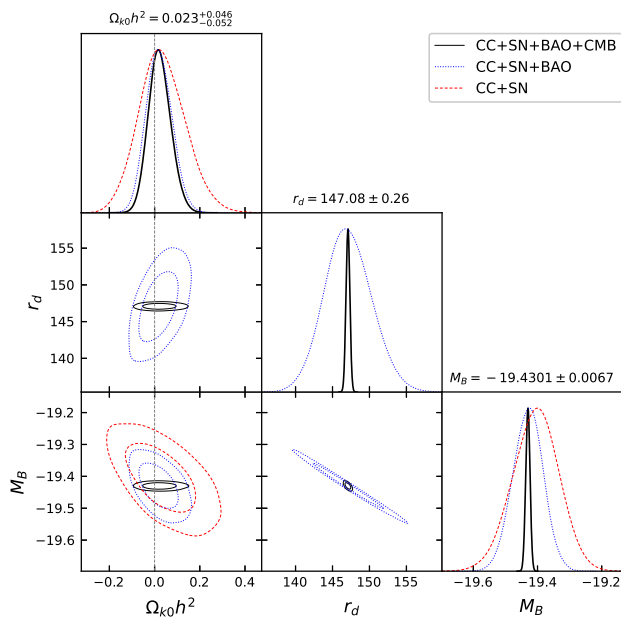


FIG. 1: Constraints on $\Omega_{k0}h^2$, r_d and M_B parameters obtained from different combinations of data. For a particular color or type, the inner and the outer contours correspond to the 1σ and 2σ confidence contours respectively. Dashed red, dotted blue, and solid black contours are obtained from CC+SN, CC+SN+BAO, and CC+SN+BAO+CMB combinations of data respectively. The constraints on the parameters are quoted in the figure for CC+SN+BAO+CMB combinations of data for which the constraints are the tightest. The vertical dashed line corresponds to $\Omega_{k0} = 0$.

	CC+SN	CC+SN+BAO	CC+SN+BAO+CMB
$\Omega_{k0}h^2$	$0.034^{+0.096}_{-0.11}$	$0.020^{+0.054}_{-0.060}$	$0.023^{+0.046}_{-0.052}$
r_d	-	147.1 ± 3.2	147.08 ± 0.26
M_B	-19.406 ± 0.072	-19.430 ± 0.047	-19.4301 ± 0.0067

TABLE I: Constraints on $\Omega_{k0}h^2$, r_d , and M_B parameters obtained from different combinations of data.

This can be seen in Table II by the comparison in Table I. We can see that the zero cosmic curvature is well within the 1σ confidence intervals for all the cases.

In Figure 3, we have shown the constraints on the GRB nuisance parameters, a , b , and σ_{ext} obtained from two combinations of data. The dotted blue and the solid-black lines are for CC+SN+BAO+GRB and CC+SN+BAO+GRB+CMB respectively. We have not explicitly shown the constraints on the $\Omega_{k0}h^2$, r_d , and M_B because these are similar as in Figure 1. This can be seen in Table III by the comparison in Table I.

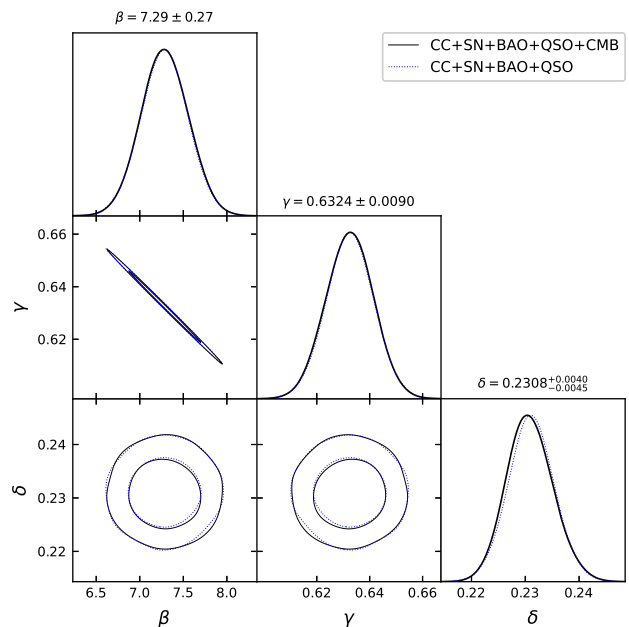


FIG. 2: Constraints on QSO data-related nuisance parameters, β , γ , and δ are obtained from two combinations of data. For a particular color or type, the inner and the outer contours correspond to the 1σ and 2σ confidence contours respectively. Dotted blue and solid black contours are obtained from CC+SN+BAO+QSO and CC+SN+BAO+QSO+CMB combinations of data respectively. The constraints on the parameters are quoted in the figure for CC+SN+BAO+QSO+CMB combinations of data.

	CC+SN+BAO+QSO	CC+SN+BAO+QSO+CMB
$\Omega_{k0}h^2$	$0.023^{+0.053}_{-0.059}$	$0.023^{+0.046}_{-0.051}$
r_d	147.1 ± 3.2	147.10 ± 0.26
M_B	-19.429 ± 0.047	-19.4307 ± 0.0065
β	7.28 ± 0.27	7.29 ± 0.27
γ	0.6326 ± 0.0089	0.6324 ± 0.0090
δ	0.2311 ± 0.0043	$0.2308^{+0.0040}_{-0.0045}$

TABLE II: Constraints on $\Omega_{k0}h^2$, r_d , M_B , β , γ , and δ parameters obtained from two different combinations of data.

From all the figures and tables, we can see that the constraints on the QSO and GRB nuisance parameters are almost independent of the constraints on the $\Omega_{k0}h^2$, r_d , and M_B .

Another important fact to notice is that constraints on all the nuisance parameters are dependent on $\Omega_{k0}h^2$ (or equivalently on $\Omega_{k0}H_0^2$) but not individually on each of Ω_{k0} and H_0 . On the other hand, we can say

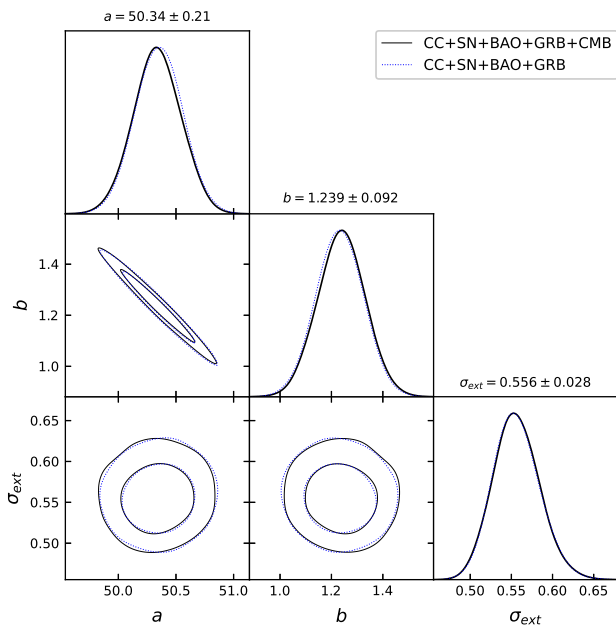


FIG. 3: Constraints on GRB data related nuisance parameters, a , b and σ_{ext} obtained from two combinations of data. For a particular color or type, the inner and the outer contours correspond to the 1σ and 2σ confidence contours respectively. Dotted blue and solid black contours are obtained from CC+SN+BAO+GRB and CC+SN+BAO+GRB+CMB combinations of data respectively. The constraint values of the parameters are quoted in the figure for CC+SN+BAO+GRB+CMB combinations of data.

	CC+SN+BAO+QSO	CC+SN+BAO+QSO+CMB
$\Omega_{k0}h^2$	0.022 ± 0.056	0.026 ± 0.050
r_d	147.1 ± 3.2	147.09 ± 0.25
M_B	-19.430 ± 0.047	-19.4304 ± 0.0066
a	50.35 ± 0.21	50.34 ± 0.21
b	1.232 ± 0.092	1.239 ± 0.092
σ_{ext}	$0.556^{+0.025}_{-0.030}$	0.556 ± 0.028

TABLE III: Constraints on $\Omega_{k0}h^2$, r_d , M_B , a , b , and σ_{ext} parameters obtained from two different combinations of data.

that we can obtain constraints only on the combination, $\Omega_{k0}H_0^2$ from all the data, considered in this analysis. To get constraints on Ω_{k0} and H_0 parameters individually, one has to add other data which directly provide observations either in H_0 or in the Ω_{k0} separately. But we are not doing this, because this is not the aim of this analysis.

This analysis concludes that we can get constraints on cosmological nuisance parameters corresponding to different observations by the different combinations of data in model independent way. This analysis has shown this fact for important observations like CC, SN, BAO, QSO, GRB, and CMB. The constraints on the nuisance parameters, obtained in this analysis, can be used as the prior for the cosmological data analysis.

Finally, we should mention that the results, obtained in this analysis, are not completely model independent. This is because there is model dependence through the Kernel and the mean function in the GPR analysis and through data like BAO and CMB which consider particular fiducial cosmological models for their results. Hence the methodology, presented here, has minimal model dependence. In the future, the GPR analysis can be replaced by more accurate, advanced, and modern reconstruction methods like neural networks to reduce the model dependence further, but the methodology, presented here, would be very helpful to do that.

* Electronic address: bikashdinda.pdf@iiserkol.ac.in

- [1] S. Perlmutter et al. (Supernova Cosmology Project), *Nature* **391**, 51 (1998), [arXiv:astro-ph/9712212](https://arxiv.org/abs/astro-ph/9712212).
- [2] A. G. Riess et al. (Supernova Search Team), *Astron. J.* **116**, 1009 (1998), [arXiv:astro-ph/9805201](https://arxiv.org/abs/astro-ph/9805201).
- [3] S. Perlmutter et al. (Supernova Cosmology Project), *Astrophys. J.* **517**, 565 (1999), [arXiv:astro-ph/9812133](https://arxiv.org/abs/astro-ph/9812133).
- [4] A. Wright, *Nature Physics* **7**, 833 (2011).
- [5] S. Linden, J. M. Virey, and A. Tilquin, *Astronomy and Astrophysics* **506**, 1095 (2009).
- [6] D. Camarena and V. Marra, *Mon. Not. Roy. Astron. Soc.* **495**, 2630 (2020), [arXiv:1910.14125 \[astro-ph.CO\]](https://arxiv.org/abs/1910.14125).
- [7] D. M. Scolnic et al. (Pan-STARRS1), *Astrophys. J.* **859**, 101 (2018), [arXiv:1710.00845 \[astro-ph.CO\]](https://arxiv.org/abs/1710.00845).
- [8] A. K. Çamlıbel, I. Semiz, and M. A. Feyizoglu, *Class. Quant. Grav.* **37**, 235001 (2020), [arXiv:2001.04408 \[astro-ph.CO\]](https://arxiv.org/abs/2001.04408).
- [9] P. A. R. Ade et al. (Planck), *Astron. Astrophys.* **571**, A16 (2014), [arXiv:1303.5076 \[astro-ph.CO\]](https://arxiv.org/abs/1303.5076).
- [10] P. A. R. Ade et al. (Planck), *Astron. Astrophys.* **594**, A13 (2016), [arXiv:1502.01589 \[astro-ph.CO\]](https://arxiv.org/abs/1502.01589).
- [11] N. Aghanim et al. (Planck), *Astron. Astrophys.* **641**, A6 (2020), [Erratum: *Astron. Astrophys.* **652**, C4 (2021)], [arXiv:1807.06209 \[astro-ph.CO\]](https://arxiv.org/abs/1807.06209).
- [12] S. Alam et al. (BOSS), *Mon. Not. Roy. Astron. Soc.* **470**, 2617 (2017),

- arXiv:1607.03155 [astro-ph.CO] .
- [13] S. Alam et al. (eBOSS), *Phys. Rev. D* **103**, 083533 (2021), arXiv:2007.08991 [astro-ph.CO] .
- [14] J. Hou et al., *Mon. Not. Roy. Astron. Soc.* **500**, 1201 (2020), arXiv:2007.08998 [astro-ph.CO] .
- [15] E. J. Copeland, M. Sami, and S. Tsujikawa, *Int. J. Mod. Phys. D* **15**, 1753 (2006), arXiv:hep-th/0603057 .
- [16] P. J. E. Peebles and B. Ratra, *Rev. Mod. Phys.* **75**, 559 (2003), arXiv:astro-ph/0207347 .
- [17] J. Yoo and Y. Watanabe, *Int. J. Mod. Phys. D* **21**, 1230002 (2012), arXiv:1212.4726 [astro-ph.CO] .
- [18] T. Clifton, P. G. Ferreira, A. Padilla, and C. Skordis, *Phys. Rept.* **513**, 1 (2012), arXiv:1106.2476 [astro-ph.CO] .
- [19] K. Koyama, *Rept. Prog. Phys.* **79**, 046902 (2016), arXiv:1504.04623 [astro-ph.CO] .
- [20] S. Tsujikawa, *Lect. Notes Phys.* **800**, 99 (2010), arXiv:1101.0191 [gr-qc] .
- [21] A. Joyce, L. Lombriser, and F. Schmidt, *Ann. Rev. Nucl. Part. Sci.* **66**, 95 (2016), arXiv:1601.06133 [astro-ph.CO] .
- [22] A. I. Lonappan, S. Kumar, Ruchika, B. R. Dinda, and A. A. Sen, *Phys. Rev. D* **97**, 043524 (2018), arXiv:1707.00603 [astro-ph.CO] .
- [23] R. Jimenez and A. Loeb, *Astrophys. J.* **573**, 37 (2002), arXiv:astro-ph/0106145 .
- [24] A. M. Pinho, S. Casas, and L. Amendola, *JCAP* **11**, 027 (2018), arXiv:1805.00027 [astro-ph.CO] .
- [25] G. Risaliti and E. Lusso, *Nature Astron.* **3**, 272 (2019), arXiv:1811.02590 [astro-ph.CO] .
- [26] E. Lusso and G. Risaliti, *Astron. Astrophys.* **602**, A79 (2017), arXiv:1703.05299 [astro-ph.HE] .
- [27] Y. Avni and H. Tananbaum, *Astrophys. J.* **305**, 83 (1986).
- [28] N. Khadka, O. Luongo, M. Muccino, and B. Ratra, *JCAP* **09**, 042 (2021), arXiv:2105.12692 [astro-ph.CO] .
- [29] H. Wei and S. N. Zhang, *Eur. Phys. J. C* **63**, 139 (2009), arXiv:0808.2240 [astro-ph] .
- [30] L. Amati, C. Guidorzi, F. Frontera, M. Della Valle, F. Finelli, R. Landi, and E. Montanari, *Mon. Not. Roy. Astron. Soc.* **391**, 577 (2008), arXiv:0805.0377 [astro-ph] .
- [31] D. H. Weinberg, M. J. Mortonson, D. J. Eisenstein, C. Hirata, A. G. Riess, and E. Rozo, *Physics Reports* **530**, 87 (2013).
- [32] M. Moresco et al., (2022), arXiv:2201.07241 [astro-ph.CO] .
- [33] S. M. Carroll, *Living Rev. Rel.* **4**, 1 (2001), arXiv:astro-ph/0004075 .
- [34] I. Zlatev, L.-M. Wang, and P. J. Steinhardt, *Phys. Rev. Lett.* **82**, 896 (1999), arXiv:astro-ph/9807002 .
- [35] V. Sahni and A. A. Starobinsky, *Int. J. Mod. Phys. D* **9**, 373 (2000), arXiv:astro-ph/9904398 .
- [36] H. Velten, R. vom Marttens, and W. Zimdahl, *Eur. Phys. J. C* **74**, 3160 (2014), arXiv:1410.2509 [astro-ph.CO] .
- [37] M. Malquarti, E. J. Copeland, and A. R. Liddle, *Phys. Rev. D* **68**, 023512 (2003), arXiv:astro-ph/0304277 .
- [38] L. Perivolaropoulos and F. Skara, *New Astron. Rev.* **95**, 101659 (2022), arXiv:2105.05208 [astro-ph.CO] .
- [39] P. Bull et al., *Phys. Dark Univ.* **12**, 56 (2016), arXiv:1512.05356 [astro-ph.CO] .
- [40] E. Di Valentino, O. Mena, S. Pan, L. Visinelli, W. Yang, A. Melchiorri, D. F. Mota, A. G. Riess, and J. Silk, (2021), arXiv:2103.01183 [astro-ph.CO] .
- [41] C. Krishnan, R. Mohayaee, E. O. Colgáin, M. M. Sheikh-Jabbari, and L. Yin, *Class. Quant. Grav.* **38**, 184001 (2021), arXiv:2105.09790 [astro-ph.CO] .
- [42] S. Vagnozzi, *Phys. Rev. D* **102**, 023518 (2020), arXiv:1907.07569 [astro-ph.CO] .
- [43] M. Chevallier and D. Polarski, *Int. J. Mod. Phys. D* **10**, 213 (2001), arXiv:gr-qc/0009008 .
- [44] E. V. Linder, *Phys. Rev. Lett.* **90**, 091301 (2003), arXiv:astro-ph/0208512 .
- [45] E. M. Barboza, Jr. and J. S. Alcaniz, *Phys. Lett. B* **666**, 415 (2008), arXiv:0805.1713 [astro-ph] .
- [46] S. Thakur, A. Nautiyal, A. A. Sen, and T. R. Seshadri, *Mon. Not. Roy. Astron. Soc.* **427**, 988 (2012), arXiv:1204.2617 [astro-ph.CO] .
- [47] B. R. Dinda, *Phys. Rev. D* **105**, 063524 (2022), arXiv:2106.02963 [astro-ph.CO] .
- [48] B. R. Dinda, *Phys. Rev. D* **100**, 043528 (2019), arXiv:1904.10418 [astro-ph.CO] .
- [49] I. Tutusaus, B. Lamine, and A. Blanchard, *Astron. Astrophys.* **625**, A15 (2019), arXiv:1803.06197 [astro-ph.CO] .
- [50] X. Zheng, S. Cao, Y. Liu, M. Biesiada, T. Liu, S. Geng, Y. Lian, and W. Guo, *Eur. Phys. J. C* **81**, 14 (2021), arXiv:2012.14607 [astro-ph.CO] .
- [51] B. L'Huilier, A. Shafieloo, E. V. Linder, and A. G. Kim, *Mon. Not. Roy. Astron. Soc.* **485**, 2783 (2019), arXiv:1812.03623 [astro-ph.CO] .
- [52] B. Wang, J.-Z. Qi, J.-F. Zhang, and X. Zhang, *Astrophys. J.* **898**, 100 (2020), arXiv:1910.12173 [astro-ph.CO] .
- [53] Y. Liu, S. Cao, T. Liu, X. Li, S. Geng, Y. Lian, and W. Guo, *Astrophys. J.* **901**, 129 (2020), arXiv:2008.08378 [astro-ph.CO] .
- [54] C. Escamilla-Rivera, M. A. C. Quintero, and S. Capozziello, *JCAP* **03**, 008 (2020), arXiv:1910.02788 [astro-ph.CO] .
- [55] M. Seikel, C. Clarkson, and M. Smith, *Journal of Cosmology and Astroparticle Physics* **2012**, 036 (2012).
- [56] A. Shafieloo, A. G. Kim, and E. V. Linder,

- [Physical Review D **85** \(2012\), 10.1103/physrevd.85.123530](#).
- [57] S.-g. Hwang, B. L'Huillier, R. E. Keeley, M. J. Jee, and A. Shafieloo, (2022), [arXiv:2206.15081 \[astro-ph.CO\]](#) .
- [58] D. Camarena and V. Marra, *Mon. Not. Roy. Astron. Soc.* **504**, 5164 (2021), [arXiv:2101.08641 \[astro-ph.CO\]](#) .
- [59] A. Gómez-Valent, *Phys. Rev. D* **105**, 043528 (2022), [arXiv:2111.15450 \[astro-ph.CO\]](#) .
- [60] S. Cao and B. Ratra, (2022), [arXiv:2203.10825 \[astro-ph.CO\]](#) .
- [61] E. O. Colgáin, M. M. Sheikh-Jabbari, R. Solomon, G. Bargiacchi, S. Capozziello, M. G. Dainotti, and D. Stojkovic, (2022), [arXiv:2203.10558 \[astro-ph.CO\]](#) .
- [62] B. R. Dinda and N. Banerjee, (2022), [arXiv:2208.14740 \[astro-ph.CO\]](#) .